

Reverso: Efficient Time Series Foundation Models for Zero-shot Forecasting

Xinghong Fu¹ Yanhong Li² Georgios Papaioannou³ Yoon Kim¹

<https://github.com/shinfxh/reverso>

Abstract

Learning time series foundation models has been shown to be a promising approach for zero-shot time series forecasting across diverse time series domains. Insofar as scaling has been a critical driver of performance of foundation models in other modalities such as language and vision, much recent work on time series foundation modeling has focused on scaling. This has resulted in time series foundation models with hundreds of millions of parameters that are, while performant, inefficient and expensive to use in practice. This paper describes a simple recipe for learning efficient foundation models for zero-shot time series forecasting that are orders of magnitude smaller. We show that large-scale transformers are not necessary: small hybrid models that interleave long convolution and linear RNN layers (in particular DeltaNet layers) can match the performance of larger transformer-based models while being more than a hundred times smaller. We also describe several data augmentation and inference strategies that further improve performance. This recipe results in *Reverso*, a family of efficient time series foundation models for zero-shot forecasting that significantly push the performance-efficiency Pareto frontier.

1. Introduction

Time series forecasting is a core problem in machine learning with widespread applications including in weather forecasting, energy grid analysis, supply chain logistics, financial predictions, and more. Traditionally, statistical models (Box & Jenkins, 1970; Engle, 1982; Bollerslev, 1986; Harvey, 1990; Hyndman & Khandakar, 2008) as well as deep learning approaches based on RNNs (Elman, 1990;

Hochreiter & Schmidhuber, 1997; Cho et al., 2014) have enjoyed great success in time series forecasting (Goel et al., 2017; Qin et al., 2017; Petneházi, 2019; Hewamalage et al., 2021, *i.a.*). More recently, models based on the transformer architecture (Vaswani et al., 2017) have led to further improvements (Nie et al., 2023; Zhou et al., 2021; Wu et al., 2021; Zhou et al., 2022; Liu et al., 2022b, *i.a.*).

These initial deep learning-based approaches to time series forecasting were dataset-specific, and thus trained models for particular domains/tasks of interest. While such models can attain high accuracy when sufficient in-distribution data are available, they incur substantial costs in data collection and model training/maintenance. This approach moreover stands in stark contrast to recent progress in domains such as language, vision, and biology, where *foundation models* pretrained on broad datasets have been found to be useful across many tasks with little or no task-specific training (Bommasani, 2021).

The successes of foundation models in other modalities have motivated the recent line of work on *time series foundation models* (TSFM; Garza et al., 2023; Ansari et al., 2024; Das et al., 2024; Liu et al., 2024; Woo et al., 2024; Liu et al., 2025b;c; Graf et al., 2025; Auer et al., 2025; Moroshan et al., 2025, *i.a.*). TSFMs are large-scale neural networks trained on heterogeneous time series data taken from broad domains (see Liang et al. (2024) and Kottapalli et al. (2025) for surveys). A particularly useful capability of decoder-based TSFMs is their ability to perform *zero-shot forecasting* via in-context learning, i.e., predicting the future given any historical time series data given as context. These TSFMs can thus serve as a domain-general tool for time series forecasting, enabling the deployment of models in domains where task-specific training data may be scarce.

However, insofar as scaling has been a critical driver of progress of foundation models in other domains, much existing work has focused on scaling TSFMs, i.e., training ever-larger models on ever-larger datasets. For example, Sun et al. (2025) train a series of models up to 1.5B parameters and observe continuous improvements with scaling model size. While such large models can be performant, their sheer size can make them prohibitively expensive to train and deploy.

¹Massachusetts Institute of Technology ²Allen Institute for AI
³Qube Research & Technologies. Correspondence to: Xinghong Fu <fxh@mit.edu>.

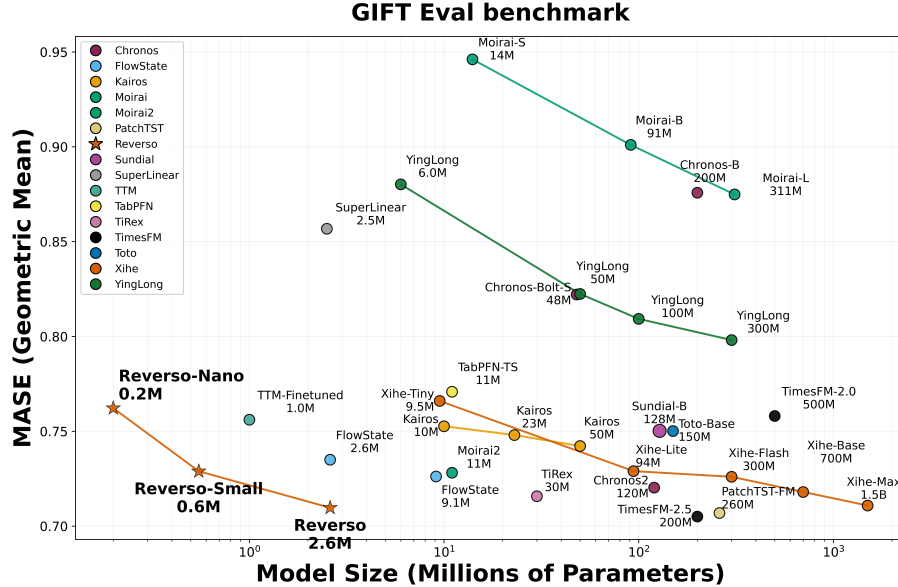


Figure 1. Zero-shot performance on the full Gift-Eval test set (Aksu et al., 2024). Reverso sets a new performance-efficiency Pareto frontier compared to existing time series foundation models.

In this work, we revisit the core assumption that large-scale models are necessary for TSFMs. We show that small models that interleave long convolution layers (Fu et al., 2023b) and modern linear RNN layers (in particular DeltaNet layers (Schlag et al., 2021; Yang et al., 2024b)) can match or outperform TSFMs that are orders of magnitude larger. We also study and ablate myriad data augmentation and inference-time strategies to arrive at a simple recipe that works well in practice. With our recipe, we train a family of TSFMs (dubbed *Reverso*) from 0.2M to 2.6M parameters that significantly push the performance-efficiency frontier, as shown in Figure 1.

2. Related Work

Time series foundation models. Our work is related to the existing research program around time series foundation models (TSFMs), which aim to train domain-general models for time series analysis and forecasting. TimeGPT (Garza et al., 2023), TimesFM (Das et al., 2024), and Lag-LLaMA (Rasul et al., 2023) were some of the first works to show that decoder-only transformers can be utilized to train TSFMs with strong zero-shot forecasting performance. Timer (Liu et al., 2024) and Timer-XL (Liu et al., 2025b) scaled such generative pretraining with dataset size, model size and context length. Moirai (Woo et al., 2024) incorporates a masked encoder to handle multivariate forecasting from various distributions. Chronos (Ansari et al., 2024) fixes the vocabulary of time series patches, while Chronos-2 (Ansari et al., 2025) introduced the group attention mechanism for multivariate forecasting. Xihe (Sun et al., 2025) scales up

TSFMs to over a billion parameters with a hierarchical block attention mechanism. PatchTST-FM-r1 (Wen et al., 2026) showed that a generic patched transformer can also achieve competitive results.

A complementary line of work reuses large language models directly for time series by reprogramming or aligning them to TS tasks (Zhou et al., 2023; Jin et al., 2023; Chang et al., 2025). However, recent studies suggest that the LLM backbone often provides little benefit over simpler LLM-free baselines (Tan et al., 2024), motivating dedicated TSFMs such as those discussed above.

Transformer alternatives for time series modeling.

While transformers have proven to be performant in the time series domain, there have also been works that employ modern “sequence-mixing” primitives—which have been shown to be effective in language modeling—for time series modeling. These works generally make use of linear attention layers (Katharopoulos et al., 2020; Peng et al., 2021; Schlag et al., 2021; Yang et al., 2024a;b), state-space models (Gu et al., 2022; Smith et al., 2023; Gu & Dao, 2024; Dao & Gu, 2024), or convolution layers (Fu et al., 2023a;b; Poli et al., 2023; Massaroli et al., 2023).

TSMamba (Ma et al., 2024) and Mamba4Cast (Bhethanabhotla et al., 2024) show that Mamba layers can be effective for time series. TiRex (Auer et al., 2025) utilizes the xlSTM (Beck et al., 2024) architecture for zero-shot forecasting, while FlowState (Graf et al., 2025) uses the S5 module (Smith et al., 2023) and operates in the coefficient space of the transformed sequence. TempoPFN (Moroshan

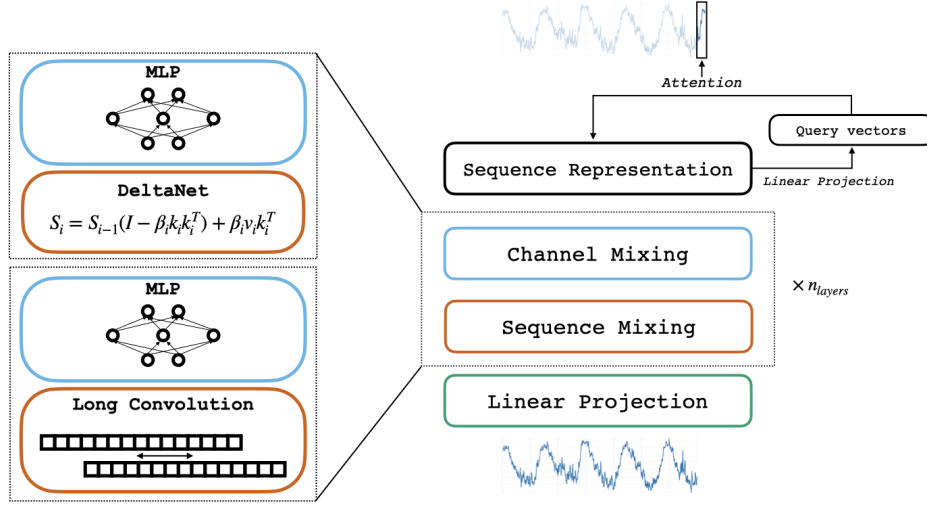


Figure 2. Reverso architecture. An input sequence $t \in \mathbb{R}^L$ of length L is first passed through a single projection layer to obtain embedding representations $x \in \mathbb{R}^{L \times d}$. Then, n_{layers} of sequence-mixing and channel-mixing blocks operates on x , where we alternate between long convolutions and DeltaNet for sequence mixing across length L , and use MLP layers for channel mixing across dimension d . The final output head (based on an attention-based transformation) obtains the predictions $\hat{y} \in \mathbb{R}^p$.

et al., 2025) makes use of the GatedDeltaProduct (Siems et al., 2025) and train on fully synthetic data. Convolution modules have been comparatively less popular in time series modeling. SCINet (Liu et al., 2022a) introduces a downsample-convolve-interact framework for modeling complex time series. ModernTCN (Luo & Wang, 2024) makes use of grouped convolutions of varying kernel sizes across multiple dimensions while TVNet (Li et al., 2025) utilizes reshaping techniques to operate on time series in three dimensions. There have also been works that show even simpler sequence mixing primitives such as linear/MLP layers work well in practice (Ekambaram et al., 2023; Wang et al., 2024; Nochumsohn et al., 2025).

3. Methods

Here we describe our recipe for learning efficient TSFMs, which includes the architecture (§3.1), dataset (§3.2), and inference strategy (§3.3). We emphasize that the individual components in our recipe are not novel: the sequence mixing primitives we use (long convolutions and DeltaNet layers) are not new; similarly, our data augmentation, synthetic data generation, and inference strategies have been proposed before in the literature. The core contribution of this work is to show that these existing ingredients can be combined to produce a TSFM that significantly pushes the performance-efficiency frontier.

3.1. Architecture

We are given an input time series $t \in \mathbb{R}^L$ of length L and must predict an output $y \in \mathbb{R}^T$ of length T . Following standard practice (Nie et al., 2023), we train by predicting a patch of p points at a time (in parallel) through learning a

function $f_\theta : \mathbb{R}^L \rightarrow \mathbb{R}^p$ parameterized with θ . During inference, we autoregressively predict chunks of p data points until we have forecasted T points. We use $L = 2048, p = 48$.

Our model architecture, shown in Figure 2, is extremely simple and consists of stacked neural network blocks where each block consists of a sequence mixing module followed by an MLP channel mixing module. Finally, we have an output decoder based on attention that uses the contextualized representation of the input to predict p data points at once.

Embedding layer. The sequence $t \in \mathbb{R}^{L \times 1}$ is first normalized within the range $[0, 1]$ with

$$t \leftarrow \frac{t - \min(t)}{\max(t) - \min(t)}.$$

We found this $[0, 1]$ -normalization to work better than z -score normalization which subtracts the mean and divides by the standard deviation.¹ In cases where there are missing values, these are imputed using linear interpolation. For sequences shorter than the model context length L , the remaining values are back-filled using the leftmost available data point.

The normalized sequence t is then up-projected pointwise using a single linear layer into d dimensions, yielding a transformed sequence $x \in \mathbb{R}^{L \times d}$. Unlike existing works that make use of special time embeddings (Moroshan et al., 2025; Alexandrov et al., 2019) to include seasonality and frequency features, utilizing metadata that might not be present at inference time, we adopt a minimalistic approach that can

¹We unnormalize the model’s output for prediction.

handle any time series as a simple numeric sequence.

Sequence mixing. We adopt a hybrid sequence mixing strategy wherein we switch between (gated) long convolution (Fu et al., 2023b) and DeltaNet layers (Schlag et al., 2021; Yang et al., 2024b).

The long convolution layer uses depthwise separable convolutions (Chollet, 2017), where the number of groups is equal to d . This obtains the output $z \in \mathbb{R}^{L \times d}$ from an input sequence $x \in \mathbb{R}^{L \times d}$ given convolution kernel weight $w \in \mathbb{R}^{k \times d}$ via

$$z_{i,j} = \sum_{m=0}^{k-1} w_{m,j} \cdot x_{i-m,j}$$

where $0 \leq i \leq L - 1$ indexes the sequence position, and $0 \leq j \leq d-1$ indexes the dimensions. The long convolution is an instance of the convolution kernel where $k = L$. This has demonstrated strong recall and reasoning performance while maintaining a sub-quadratic compute cost (Poli et al., 2023). We also make use of a gating layer, where the gate comes from a depthwise separable (short) convolution layer. Taken together, our convolutional sequence mixing primitive is given by

$$\begin{aligned} x_{conv} &\leftarrow \text{SiLU}(\text{short-conv}(x) \odot \text{long-conv}(x)) \\ x &\leftarrow x + \text{LayerNorm}(x_{conv}). \end{aligned}$$

With FFT the overall complexity of the convolution layer is $O(dL \log L)$, enabling faster training than standard attention. While the FFT-based convolutions was previously not optimized for GPUs, recent works have enabled significant wallclock speed-ups (Fu et al., 2023b), which we make use of in practice.

We also make use of linear RNN layers every other layer. The particular instance used in Reverso is DeltaNet (Schlag et al., 2021). DeltaNet learns the following state transition using query, key and value vectors $q_i, k_i, v_i \in \mathbb{R}^{d_h}$ (with head dimension d_h)

$$\begin{aligned} S_i &= S_{i-1}(I - \beta_i k_i k_i^T) + \beta_i v_i k_i^T \\ x_i &\leftarrow x_i + \text{LayerNorm}(S_i q_i) \end{aligned}$$

where the query, key, value vectors are obtained from linear projections followed by short convolutions of the input x , and $\beta_i \in (0, 1)$ is obtained by a linear projection of the input x_i followed by a sigmoid. We use 4 heads (i.e., $d_h = \frac{d}{4}$). To better model bidirectional context over the entire length L sequence, we add the last time step of the previous layer to the current layer’s first hidden state (i.e., $x_0^{(l)} \leftarrow x_0^{(l)} + x_{L-1}^{(l-1)}$) before the DeltaNet layer. We found this type of vector-based “state-weaving” strategy to work well in practice. Similar state-weaving strategies have been explored in Moroshan et al. (2025).

In our ablation studies we also compare against other DeltaNet variants such as Gated DeltaNet (GDN; Yang et al., 2025) and Gated Delta Product (GDP; Siems et al., 2025), as well as linear attention variants such Gated Linear Attention (GLA; Yang et al., 2024a) (which generalizes state-space models such as Mamba-2 (Dao & Gu, 2024)). Our findings show that DeltaNet performs well despite having fewer parameters.

Channel mixing. Each sequence mixing layer is followed by a channel mixing MLP layer. The MLP layer works as in the standard transformer architecture (Vaswani et al., 2017), with a dimension expansion factor of 4, with ReLU activations:

$$\begin{aligned} x_{mlp} &\leftarrow \text{ReLU}(xW_{up})W_{down} \\ x &\leftarrow x + \text{LayerNorm}(x_{mlp}) \end{aligned}$$

We found this simple MLP to work better than GLU-based alternatives (Shazeer, 2020).

Decoder head. The above blocks transform a sequence of inputs $x^{(0)} \in \mathbb{R}^{L \times d}$ into $x^{(n)} \in \mathbb{R}^{L \times d}$ after n layers. To obtain the final prediction, we first pass the final transformed input $x^{(n)}$ to obtain a set of decoder “query” vectors q_{dec} :

$$\begin{aligned} z &= W_L x^{(n)}, & W_L \in \mathbb{R}^{p \times L}, z \in \mathbb{R}^{p \times d} \\ q_{dec} &= zW_q, & W_q \in \mathbb{R}^{d \times d}, q_{dec} \in \mathbb{R}^{p \times d} \end{aligned}$$

The decoder query vectors are then used to attend over the keys and values obtained from a transformation over $x^{(n)}$,

$$\begin{aligned} k_{dec} &= x^{(n)}W_k, & W_k \in \mathbb{R}^{d \times d}, \\ v_{dec} &= x^{(n)}W_v, & W_v \in \mathbb{R}^{d \times d}, \\ o &= \text{attention}(q_{dec}, k_{dec}, v_{dec}), & o \in \mathbb{R}^{p \times d}. \end{aligned}$$

We find that smaller models train well without any positional embedding, whereas `sin-cos` positional embedding improves performance for Reverso-2.6M. Finally, we apply a linear layer to obtain the final output $\hat{y} \in \mathbb{R}^p$:

$$\hat{y} = z w_o, \quad w \in \mathbb{R}^{d \times 1}.$$

We found this type of attention-based decoder “head” to be more performant and parameter-efficient than a simple linear layer that directly predicts a p -sized vector from $x^{(n)}$.

Training objective. Given the model prediction \hat{y} we unnormalized the output and train against the ground truth output y , using the mean absolute error (MAE) loss, where we masked out NaN values on the ground truth y during loss computation.

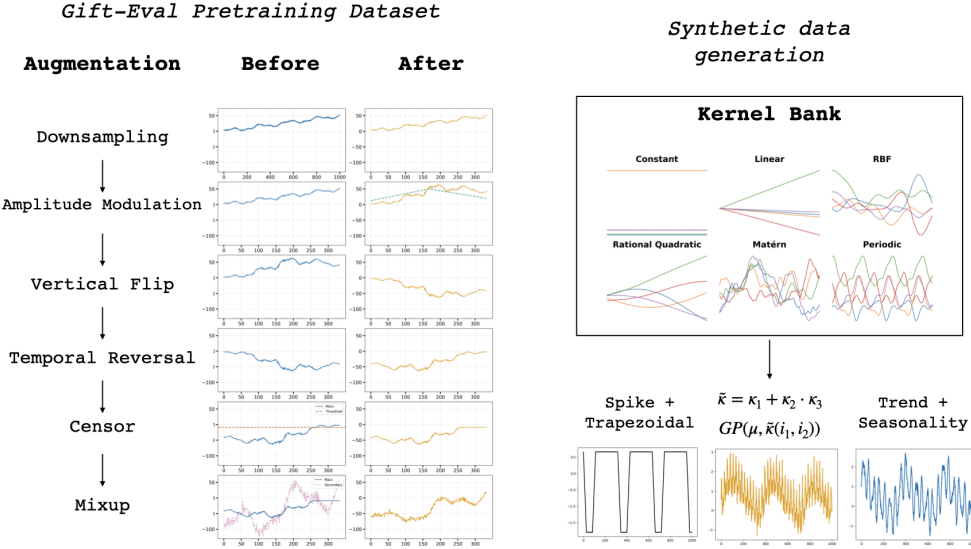


Figure 3. Our data augmentation (left) and synthetic data generation (right) pipeline. For data augmentation we apply a series of standard data augmentations: downsampling, amplitude modulation, vertical flip, horizontal flip, censor, mixup. For synthetic data generation, we generate data from Gaussian process with randomly selected kernels from a kernel bank, and combine this with spike/trapezoidal patterns as well as processes sampled with trend, seasonality and irregularity.

3.2. Dataset

Here we describe the pretraining dataset in addition to strategies for data augmentation and synthetic data generation.

Pretraining dataset. The time series community has developed a series of commonly-used datasets (Godahewa et al., 2021; Alexandrov et al., 2019; Aksu et al., 2024; Woo et al., 2024), consisting of data from various sources such as weather, traffic, and other domains. We train our models on the GiftEval (Aksu et al., 2024) pretraining dataset, which has become the de facto standard for training TSFMs in recent years. The GiftEval pretraining dataset has around 4.5 million time series with 230 billion time points in total. The dataset however is significantly imbalanced towards datasets such as Buildings900k (Emami et al., 2024), and Era5 (Hersbach et al., 2020).

To resolve this dataset imbalance, we precompute the strides on each dataset necessary to achieve a target (roughly uniform) fraction of time series sampled. For each dataset, we target a maximum of $N_{max} = 100000$ samples per epoch, and recompute the strides such that we have at most N_{max} samples from each dataset. Explicitly, for each dataset \mathcal{D} with time series samples $t \in \mathcal{D}$ each of length l_t , we compute the total sum of lengths as $\sum_{t \in \mathcal{D}} l_t$, and compute the stride for this dataset as $s_{\mathcal{D}} = \left\lceil \frac{\sum_{t \in \mathcal{D}} l_t}{N_{max}} \right\rceil$. We also set an upper limit to 48 samples per time series t , to avoid oversampling short datasets. A random start point in each sequence

t is chosen at each epoch to ensure sampling across the full pretraining set.

Data augmentation. Several techniques for data augmentation have been previously reported to help increase data diversity during pretraining TSFMs. We explored these augmentation techniques and found the following to be useful, which we eventually incorporated into our pretraining recipe: downsampling, amplitude modulation, flip along the x and y -axis (i.e., sign inversion and temporal reversal in Moroshan et al. (2025)), censor augmentation and mixup (Ansari et al., 2024), applied in this order. See Figure 3 (left). Downsampling and amplitude modulation are applied at the level of the full sequence. Flip augmentations and censor augmentations are applied on each subsampled sequence of context length L and mixup is applied to the full batch. The full data augmentation pipeline is given in Algorithm 4 of the appendix.

Synthetic data. We use synthetic data similar to established baselines (Auer et al., 2025; Ansari et al., 2024), using methods such KernelSynth (Ansari et al., 2024), which use Gaussian processes to generate synthetic data. In particular, we define a kernel bank \mathcal{K} (see Table 8 of the appendix), and sample $j \sim U\{1, 5\}$ kernels from \mathcal{K} and compose them using random binary additive or multiplicative operations. This forms a composite kernel $\tilde{\kappa}$. We also sample a mean μ which follows a linear trend with slope $m \sim U[-0.01, 0.01]$ and intercept $c \sim U[-1, 1]$ with probability 1/2 and con-

stant otherwise. We then use $\tilde{\kappa}$ and μ in a Gaussian process to sample the synthetic time series t_{syn} . See Figure 3 (right).

We also include spike processes (Auer et al., 2025; Moshyan et al., 2025; Feng et al., 2025) and TSI (Bahrpeyma et al., 2021) as used in Chronos-2 to help in learning simple trends and periodic patterns, as further described in Algorithms 2 and 3 of the appendix. We generate a total of 1 million synthetic time series sequences with the above algorithm. The maximum sequence length is set to 4096.

3.3. Inference

We apply several techniques at inference time that help improve performance.

Flip equivariance. Following prior works (Das et al., 2024), we found it helpful to ensure flip equivariance by passing both the original and flipped context to the model, and then averaging the results:

$$\hat{y} = \frac{f(x) - f(-x)}{2}$$

While this requires two forward passes of the model, we observe that this reduces forecasting error consistently across multiple benchmarks.

Downsampling. Given a pretrained TSFM with fixed context length L , we generally want to ensure that patterns we wish to capture in the time series have seasonality period $S < L$. The case of $S > L$ potentially results in insufficient information for an effective forecast. Works such as Flowstate (Graf et al., 2025) determine this downsampling factor by rescaling the series with a ratio between the seasonality of the data and a base seasonality of the model. However, such an approach relies heavily on the metadata of the input that might not be available at inference time, and requires the handling of several edge cases where multiple frequency scales are present.

We instead use a simple algorithm to determine the downsampling factors using FFT as described below. We first compute the Fast Fourier Transform (FFT) of the input sequence $t \in \mathbb{R}^L$ to obtain the amplitude spectrum $A(f)$. We then identify the peaks in the spectrum. To distinguish the dominant peak from noise, we enforce a set of criteria, as described in Algorithm 5 and Appendix D.

Sequences t where the seasonality exceeds the context length L of Reverso are downsampled by a factor of k to t' which is passed as input to the model. Given an original forecast horizon L , the model now predicts $\lceil L/k \rceil$ timesteps, which are then upsampled to L by linear interpolation. An intuitive illustration is shown in Figure 7 of the appendix.

Table 1. Architecture configurations for Reverso models of different sizes.

Model	Parameters	Layers	Dim (d)
Reverso-Nano	200K	2	32
Reverso-Small	550K	4	64
Reverso	2.6M	8	128

4. Empirical Study

4.1. Experimental Setup

We pretrain three versions of Reverso with 200K, 550K and 2.6M parameters. See Table 1 for the model configurations. We train with AdamW (Loshchilov & Hutter, 2019) with maximum learning rate 5×10^{-4} using a WSD scheduler (Wen et al., 2025), $\beta_1 = 0.9$, $\beta_2 = 0.999$, $\epsilon = 1 \times 10^{-8}$ and weight decay of 0.1 and we roughly sample 1 million time points per training step with a batch size of 512. Our models take $\{10, 20, 40\}$ H100-hours for a full training run.

Baselines. Our baselines include state-of-the-art TSFMs across varying architectures and sizes: Chronos and Chronos-2 (Ansari et al., 2024; 2025), TimesFM-2 and TimesFM-2.5 (Das et al., 2024), PatchTST-FM-r1 (Wen et al., 2026), TiRex (Auer et al., 2025), FlowState (Graf et al., 2025), Xihe (Sun et al., 2025), Kairos (Feng et al., 2025), Moirai and Moirai-2 (Woo et al., 2024; Liu et al., 2025a), Sundial (Liu et al., 2025c), Toto (Cohen et al., 2025), YingLong (Wang et al., 2025) and Tiny-time Mixers (Ekambaram et al., 2024). The sizes of these baseline models are given in Figure 1 and Figure 4.

4.2. Main Results: Zero-Shot Forecasting Performance

Gift-Eval. The Gift-Eval benchmark (Aksu et al., 2024) contains 23 different datasets with 97 different forecasting tasks. We train with the provided Gift-Eval Pretrain dataset.² On this benchmark, Reverso achieves a competitive MASE value of 0.711 at a modest model size of 2.6M parameters. In particular, we outperform similarly small TSFMs such as Super-Linear (2.5M), FlowState (2.6M) and Tiny-Time Mixers (1M).³ Reverso-Small, at just 550K parameters, outperforms all the above models with an MASE of 0.726. Table 9 of the appendix gives the full numeric results broken down by dataset/domain, while Figure 6 shows some qualitative results on various datasets. We visualize the results for the full benchmark for all models in Figure 1 (see Table 10 of the appendix for the full table of baselines and their results).

²<https://huggingface.co/datasets/Salesforce/GiftEvalPretrain>

³The official zero-shot performance of pretrained TTM-R2 lags significantly behind other baselines (MASE=1.02), so we compare against a stronger finetuned model (TTM-R2-Finetuned) which achieves MASE of 0.756.

Table 2. Model MASE scores across forecast horizons, averaged across the 21 datasets in Gift-Eval with all three horizons available. Our Reverso models demonstrate strong long horizon forecasting abilities, despite the multiple autoregressive rollouts using our prediction length of 48 as compared to models like Xihe-Max with maximum prediction length of 720.

Model	Params	MASE		
		Short	Medium	Long
Xihe-Max	1.5B	0.623	0.718	0.763
TimesFM-2.5	200M	0.626	0.724	0.751
PatchTST-FM	260M	0.616	0.722	0.745
TiRex	30M	0.638	0.750	0.767
Reverso	2.6M	0.633	0.705	0.749
Reverso-Small	550K	0.648	0.728	0.754

We also observe that our model does particularly well in long sequence forecasting. Table 2 shows the performance of the top TSFs on each of the short/medium/long horizon splits within Gift-Eval, where we see that Reverso achieves strong medium and long horizon point forecasting results, despite being the smallest family of models evaluated on this benchmark.

LTSF/TSLib. We next explore zero-shot transfer results to the LTSF (Zeng et al., 2023) test set. On this dataset we outperform Sundial (Liu et al., 2025c), Super-Linear (Nochumsohn et al., 2025), Timer-XL (Liu et al., 2025b) and several other models at a much smaller parameter count, as shown in Figure 4. We report more granular performance numbers in Table 3, where we follow Sundial (Liu et al., 2025c) and report the mean MAE achieved across various prediction horizons for the datasets of ETTh1, ETTh2, ETTm1, ETTm2, Electricity and Weather.

These results are especially strong given that some of the baselines are quite advantaged compared to Reverso. For example, in-domain datasets such as Electricity enter into the pretraining datasets of TiRex and Chronos-2. Moreover, for models which do not report results on the full benchmark, we impute their scores with the best existing model on each missing dataset.⁴ Despite the advantage given to all other models, we observe that Reverso is still the one of the best performing class of models on LTSF.

4.3. Ablations

We perform ablations across various architectural, dataset, and inference-strategy choices.

Architecture. How much does our hybrid sequence mixing layers help for time series? In Table 4, we report the MASE achieved by different instances of our model using

⁴For instance, the values for Electricity for YingLong were imputed using the MAE values obtained by Chronos-2.

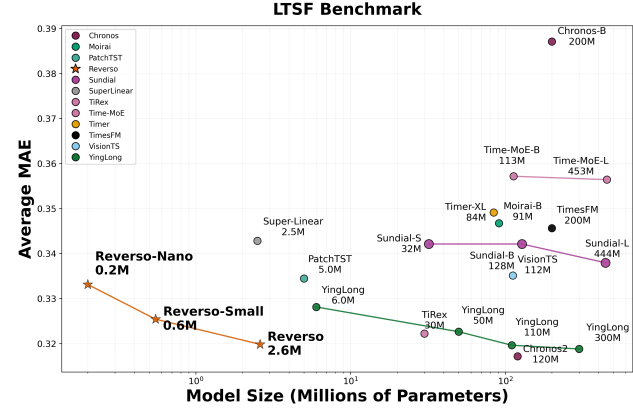


Figure 4. LTSF performance vs. Parameter Count. MAE is averaged over the horizons of {96, 192, 336, 720} for the datasets ETTh1, ETTh2, ETTm1, ETTm2, Electricity and Weather. For models which are not evaluated on all the datasets (e.g. YingLong did not report results for Electricity), we impute with the other best existing model on that dataset.

the different sequence mixing layers. Across each model, we keep the number of layers fixed at 8 and sequence mixing dimension at 128. Here we train on a smaller portion of the full training set for efficiency.

We find that for non-hybrid models, DeltaNet (Schlag et al., 2021) and Gated DeltaNet (Yang et al., 2025) achieves the low loss with few parameter counts compared to layers like Gated Linear Attention (Yang et al., 2024a) and DeltaProduct (Siems et al., 2025). Overall, linear attention and convolution methods consistently outperform full attention. Hybrid models that combine long convolutions with linear RNN layers ultimately perform best.

Table 5 shows ablation studies on our attention decoder head, where we replace the attention mechanism with a simple (bi)linear layer. For the simple linear layer, the hidden states $x^{(n)} \in \mathbb{R}^{L \times d}$ after the last Reverso block are projected to the output with two linear projections $W_1 \in \mathbb{R}^{d \times 1}$ and $W_2 \in \mathbb{R}^{p \times L}$ with the following transformation

$$\hat{y} = W_2 x^{(L)} W_1.$$

We observe that the attention mechanism at the decoder boosts overall performance, in particular helps to capture long range dependencies.

Data augmentation and synthetic data. Data augmentation strategies and synthetic data generation processes have been shown to improve data diversity. Table 6 shows a leave-one-out experiment, where we train Reverso (again on a smaller training set) while removing each one of the data augmentations within the pipeline {mixup, downsample, temporal reversal(flip-x), vertical flip(flip-y), censor, amplitude modulation}. We find that our

Table 3. Zero-shot forecasting performance (MAE) on LTSF datasets: ETTm1, ETTm2, ETTh1, ETTh2, Electricity and Weather, comparing between Reverso variants against state-of-the-art foundation models. Results represent the averaged MAE across prediction lengths {96, 192, 336, 720}. Best results are in **bold**, and second-best are underlined. A full set of results are shown in Table 12

Model	Reverso	Reverso-Small	Reverso-Nano	Sundial-L	Super-Linear	Timer-XL	TiRex	Chronos-2
Params	2.6M	550K	200K	444M	2.6M	85M	30M	120M
ETTm1	0.367	0.376	0.382	0.369	0.389	0.392	<u>0.365</u>	0.359
ETTm2	0.304	0.309	0.311	0.315	0.325	0.336	<u>0.302</u>	0.291
ETTh1	0.404	0.404	0.416	0.420	0.416	0.417	0.417	0.405
ETTh2	<u>0.365</u>	0.370	0.384	0.387	0.386	0.388	0.362	0.367
Electricity	<u>0.238</u>	0.241	0.249	0.262	0.267	0.268	0.240	0.237
Weather	0.253	0.252	0.257	0.275	0.275	0.294	<u>0.247</u>	0.245
Avg	<u>0.322</u>	0.325	0.333	0.338	0.343	0.349	<u>0.322</u>	0.317
Avg Rank	<u>2.50</u>	3.83	5.17	6.33	6.17	7.83	2.83	1.67

Table 4. Sequence mixing layer ablations for Reverso, at the same 8 layer 128 dimension setting. Results are shown for Gift-Eval.

Sequence Module	Params	Long MASE	Short MASE	Overall MASE
DeltaNet	2.0M	0.706	0.792	0.732
Gated DeltaProduct	3.0M	0.711	0.793	0.735
Gated DeltaNet	2.6M	0.708	0.782	0.730
Long Convolution	3.1M	0.708	0.799	0.735
Gated Linear Attention	2.1M	0.726	0.817	0.753
Attention (sin-cos)	2.0M	0.729	0.840	0.762
Attention (RoPE)	2.0M	0.719	0.824	0.750
Conv + Gated DeltaNet	3.1M	0.704	0.784	0.728
Conv + DeltaNet (Reverso)	2.6M	0.700	0.786	0.725

Table 5. Decoder head ablations, using different sizes of Reverso. We compare the use of attention mechanism within the decoder head against a simple bilinear output layer.

Decoder Architecture	Reverso Layers	Dimension	Long MASE	Short MASE	Overall MASE
Linear	4	64	0.751	0.830	0.774
Attention	4	64	0.728	0.811	0.753
Linear	8	128	0.719	0.789	0.740
Attention	8	128	0.700	0.786	0.725

training recipe is robust to the setting of individual data augmentation techniques, where removing a single data augmentation does not significantly hurt pre-training. But at the same time, the usage of augmentations remain necessary, and ablating them altogether is detrimental. Synthetic data also shows significant benefit, even when present in small ratios. This finding corroborates recent works (Ansari et al., 2025; Moroshan et al., 2025) which also highlight the importance of data augmentations and synthetic data in training TSFMs.

Inference. Finally, we analyze the different effects of downsampling and flip invariance methods described in Section 3.3 in forecasting. We find that downsampling helps

Table 6. Ablations on dataset augmentation and synthetic data.

Method	MASE
Baseline	0.738
w/o mixup	0.740
w/o downsample	0.740
w/o temp rev	0.740
w/o flip	0.739
w/o censor	0.738
w/o amp mod	0.737
w/o any data augmentation	0.755
w/o synthetic data	0.786

Table 7. Ablations on inference strategy on Gift-Eval.

Method	Short Seq	Long Seq	Short Term	Med Term	Long Term	Overall
Baseline	0.781	0.697	0.710	0.730	0.746	0.722
w/o downsampling	0.781	0.717	0.710	0.755	0.789	0.736
No flip	0.788	0.700	0.715	0.730	0.748	0.726
Flip once	0.781	0.698	0.710	0.730	0.747	0.722
Flip every	0.781	0.697	0.710	0.730	0.746	0.722

bring long range dependencies into the context window of our model, improving the medium and long term forecast performance.

Flip invariance helps more on short sequences. We compare two methods of doing this autoregressive rollout: `flip-once` where the original and flipped predictions across the whole forecast horizon are obtained separately and averaged once at the end after the autoregressive rollout is completed, versus `flip-every` where the original and flipped predictions are averaged at the end of each intermediate autoregressive step. The latter method shows slightly more marginal improvements than the former.

5. Discussion

As stated in §3, Reverso is built from established architectural components; our main contribution lies in how we combine them. We show that recent hybrid models that have been successful in language modeling can result in simple TSFMs that yield a strong performance–efficiency trade-off.

More generally, we view Reverso as an optimized recipe for TSFMs. Similar patterns have appeared in foundation models in other domains: RoBERTa (Liu et al., 2019) systematically refines the original BERT recipe (Devlin et al., 2019), while DINOv2 (Oquab et al., 2023) streamlines the original DINO formulation. Likewise, many influential works in foundation modeling arise from scaling up existing designs (e.g., GPT-2 to GPT-3), rather than introducing entirely new building blocks. Our results show that, in the TSFM setting, carefully designed architectures allow us instead to *scale down* existing recipes while maintaining competitive performance, effectively pushing the Pareto frontier towards smaller and cheaper models. Our findings also resonate with recent work on hybrid LLM architectures (Lieber et al., 2024; Glorioso et al., 2024; Waleffe et al., 2024), which demonstrates that mixing established primitives can outperform either component alone.

Reverso still has several limitations. First, Reverso is trained primarily as a univariate forecasting model. Chronos-2 has shown that attention can be cleverly utilized to learn cross-channel dependence in multivariate time series. Future work could investigate the potentials of the various sequence mixing layers in multivariate domains. Second, while Reverso’s performance on long sequence was near state-of-the-art, its performance on shorter sequences still lagged behind larger TSFMs. Finally, we focus primarily on point prediction, although some applications of interest would benefit from distributional predictions; insofar as conformal methods (Stankeviciute et al., 2021; Sun & Yu, 2025) have also been adopted as a lightweight adaptation to obtain uncertainty bounds for any point time series forecasts, we anticipate such techniques being applicable to obtain uncertainty estimates from Reverso models.

6. Conclusion

This paper presents Reverso, a family of models that significantly push the efficiency–performance frontier of TSFMs. We show that large-scale models are not necessary, and that simple architectures based on convolutions and linear RNN layers can achieve competitive zero-shot forecasting performance. Reverso demonstrates strong capability as a highly accurate model for long sequence, long horizon forecasting.

Impact Statement

This paper presents work whose goal is to advance the field of Machine Learning. There are many potential societal consequences of our work, none of which we feel must be specifically highlighted here.

Acknowledgments

This work was supported by the National Science Foundation under CAREER Award No. 2441872 and a gift from Qube RT.

References

Aksu, T., Woo, G., Liu, J., Liu, X., Liu, C., Savarese, S., Xiong, C., and Sahoo, D. Gift-eval: A benchmark for general time series forecasting model evaluation, 2024. URL <https://arxiv.org/abs/2410.10393>.

Alexandrov, A., Benidis, K., Bohlke-Schneider, M., Flunkert, V., Gasthaus, J., Januschowski, T., Maddix, D. C., Rangapuram, S., Salinas, D., Schulz, J., Stella, L., Türkmen, A. C., and Wang, Y. Gluonts: Probabilistic time series models in python, 2019. URL <https://arxiv.org/abs/1906.05264>.

Ansari, A. F., Stella, L., Türkmen, C., Zhang, X., Mercado, P., Shen, H., Shchur, O., Rangapuram, S. S., Arango, S. P., Kapoor, S., Zschiegner, J., Maddix, D. C., Wang, H., Mahoney, M. W., Torkkola, K., Wilson, A. G., Bohlke-Schneider, M., and Wang, Y. Chronos: Learning the language of time series, 2024. URL <https://arxiv.org/abs/2403.07815>.

Ansari, A. F., Shchur, O., Küken, J., Auer, A., Han, B., Mercado, P., Rangapuram, S. S., Shen, H., Stella, L., Zhang, X., Goswami, M., Kapoor, S., Maddix, D. C., Guerron, P., Hu, T., Yin, J., Erickson, N., Desai, P. M., Wang, H., Rangwala, H., Karypis, G., Wang, Y., and Bohlke-Schneider, M. Chronos-2: From univariate to universal forecasting, 2025. URL <https://arxiv.org/abs/2510.15821>.

Auer, A., Podest, P., Klotz, D., Böck, S., Klambauer, G., and Hochreiter, S. Tirex: Zero-shot forecasting across long and short horizons with enhanced in-context learning. In *The Thirty-ninth Annual Conference on Neural Information Processing Systems*, 2025. URL <https://openreview.net/forum?id=v7UqniC9pF>.

Bahrpeyma, F., Roantree, M., Cappellari, P., Scriney, M., and McCarren, A. A methodology for validating diversity in synthetic time series generation. *MethodsX*, 8:101459, 2021. ISSN 2215-0161. doi: <https://doi.org/10.1016/j.mex.2021.101459>.

Beck, M., Pöppel, K., Spanring, M., Auer, A., Prudnikova, O., Kopp, M. K., Klambauer, G., Brandstetter, J., and Hochreiter, S. xLSTM: Extended long short-term memory. In *The Thirty-eighth Annual Conference on Neural Information Processing Systems*, 2024. URL <https://openreview.net/forum?id=ARAxPPIAhq>.

Bhethanabhotla, S. K., Swelam, O., Siems, J., Salinas, D., and Hutter, F. Mamba4cast: Efficient zero-shot time series forecasting with state space models. *arXiv preprint arXiv:2410.09385*, 2024.

Bollerslev, T. Generalized autoregressive conditional heteroskedasticity. *Journal of Econometrics*, 31(3):307–327, 1986.

Bommasani, R. On the opportunities and risks of foundation models. *arXiv preprint arXiv:2108.07258*, 2021.

Box, G. E. P. and Jenkins, G. M. *Time Series Analysis: Forecasting and Control*. Holden-Day, 1970.

Chang, C., Wang, W.-Y., Peng, W.-C., and Chen, T.-F. Llm4ts: Aligning pre-trained llms as data-efficient time-series forecasters. *ACM Transactions on Intelligent Systems and Technology*, 16(3):1–20, 2025.

Cho, K., Van Merriënboer, B., Gulcehre, C., Bahdanau, D., Bougares, F., Schwenk, H., and Bengio, Y. Learning phrase representations using rnn encoder-decoder for statistical machine translation. *arXiv preprint arXiv:1406.1078*, 2014.

Chollet, F. Xception: Deep learning with depthwise separable convolutions, 2017. URL <https://arxiv.org/abs/1610.02357>.

Cohen, B., Khwaja, E., Doubli, Y., Lemaachi, S., Lettieri, C., Masson, C., Miccinilli, H., Ramé, E., Ren, Q., Rostamizadeh, A., du Terrain, J. O., Toon, A.-M., Wang, K., Xie, S., Xu, Z., Zhukova, V., Asker, D., Talwalkar, A., and Abou-Amal, O. This time is different: An observability perspective on time series foundation models, 2025. URL <https://arxiv.org/abs/2505.14766>.

Dao, T. and Gu, A. Transformers are ssms: Generalized models and efficient algorithms through structured state space duality. In *Proceedings of ICML*, 2024.

Das, A., Kong, W., Sen, R., and Zhou, Y. A decoder-only foundation model for time-series forecasting, 2024. URL <https://arxiv.org/abs/2310.10688>.

Devlin, J., Chang, M.-W., Lee, K., and Toutanova, K. Bert: Pre-training of deep bidirectional transformers for language understanding. In *Proceedings of NAACL-HLT*, pp. 4171–4186, 2019.

Ekambaram, V., Jati, A., Nguyen, N., Sinthong, P., and Kalagnanam, J. Tsmixer: Lightweight mlp-mixer model for multivariate time series forecasting. In *Proceedings of the 29th ACM SIGKDD conference on knowledge discovery and data mining*, pp. 459–469, 2023.

Ekambaram, V., Jati, A., Dayama, P., Mukherjee, S., Nguyen, N. H., Gifford, W. M., Reddy, C., and Kalagnanam, J. Tiny time mixers (ttms): Fast pre-trained models for enhanced zero/few-shot forecasting of multivariate time series, 2024. URL <https://arxiv.org/abs/2401.03955>.

Elman, J. L. Finding structure in time. *Cognitive Science*, 14(2):179–211, 1990.

Emami, P., Sahu, A., and Graf, P. Buildingsbench: A large-scale dataset of 900k buildings and benchmark for short-term load forecasting, 2024. URL <https://arxiv.org/abs/2307.00142>.

Engle, R. F. Autoregressive conditional heteroscedasticity with estimates of the variance of united kingdom inflation. *Econometrica*, 50(4):987–1007, 1982.

Feng, K., Lan, S., Fang, Y., He, W., Ma, L., Lu, X., and Ren, K. Kairos: Towards adaptive and generalizable time series foundation models, 2025. URL <https://arxiv.org/abs/2509.25826>.

Fu, D. Y., Dao, T., Saab, K. K., Thomas, A. W., Rudra, A., and Ré, C. Hungry Hungry Hippos: Towards language modeling with state space models. In *International Conference on Learning Representations*, 2023a.

Fu, D. Y., Epstein, E. L., Nguyen, E., Thomas, A. W., Zhang, M., Dao, T., Rudra, A., and Ré, C. Simple hardware-efficient long convolutions for sequence modeling. *International Conference on Machine Learning*, 2023b.

Garza, A., Challu, C., and Mergenthaler-Canseco, M. Timegpt-1. *arXiv preprint arXiv:2310.03589*, 2023.

Glorioso, P., Anthony, Q., Tokpanov, Y., Whittington, J., Pilault, J., Ibrahim, A., and Millidge, B. Zamba: A compact 7b ssm hybrid model. *arXiv preprint arXiv:2405.16712*, 2024.

Godahewa, R., Bergmeir, C., Webb, G. I., Hyndman, R. J., and Montero-Manso, P. Monash time series forecasting archive, 2021. URL <https://arxiv.org/abs/2105.06643>.

Goel, H., Melnyk, I., and Banerjee, A. R2n2: Residual recurrent neural networks for multivariate time series forecasting. *arXiv preprint arXiv:1709.03159*, 2017.

Graf, L., Ortner, T., Woźniak, S., and Pantazi, A. Flowstate: Sampling rate invariant time series forecasting, 2025. URL <https://arxiv.org/abs/2508.05287>.

Gu, A. and Dao, T. Mamba: Linear-time sequence modeling with selective state spaces. In *Proceedings of CoLM*, 2024.

Gu, A., Goel, K., and Ré, C. Efficiently modeling long sequences with structured state spaces. In *Proceedings of ICLR*, 2022.

Harvey, A. C. *Forecasting, Structural Time Series Models and the Kalman Filter*. Cambridge University Press, Cambridge, 1990.

Hersbach, H., Bell, B., Berrisford, P., Hirahara, S., Horányi, A., Muñoz-Sabater, J., Nicolas, J., Peubey, C., Radu, R., Schepers, D., Simmons, A., Soci, C., Abdalla, S., Abellán, X., Balsamo, G., Bechtold, P., Biavati, G., Bidlot, J., Bonavita, M., De Chiara, G., Dahlgren, P., Dee, D., Diamantakis, M., Dragani, R., Flemming, J., Forbes, R., Fuentes, M., Geer, A., Haimberger, L., Healy, S., Hogan, R. J., Hólm, E., Janisková, M., Keeley, S., Laloyaux, P., Lopez, P., Luptu, C., Radnoti, G., de Rosnay, P., Rozum, I., Vamborg, F., Villaume, S., and Thépaut, J.-N. The ERA5 global reanalysis. *Quarterly Journal of the Royal Meteorological Society*, 146(730):1999–2049, 2020. doi: <https://doi.org/10.1002/qj.3803>. URL <https://rmets.onlinelibrary.wiley.com/doi/abs/10.1002/qj.3803>.

Hewamalage, H., Bergmeir, C., and Bandara, K. Recurrent neural networks for time series forecasting: Current status and future directions. *International Journal of Forecasting*, 37(1):388–427, 2021.

Hochreiter, S. and Schmidhuber, J. Long short-term memory. *Neural Computation*, 9(8):1735–1780, 1997.

Hyndman, R. J. and Khandakar, Y. Automatic time series forecasting: The forecast package for r. *Journal of Statistical Software*, 27(3):1–22, 2008.

Jin, M., Wang, S., Ma, L., Chu, Z., Zhang, J. Y., Shi, X., Chen, P.-Y., Liang, Y., Li, Y.-F., Pan, S., et al. Time-llm: Time series forecasting by reprogramming large language models. *arXiv preprint arXiv:2310.01728*, 2023.

Katharopoulos, A., Vyas, A., Pappas, N., and Fleuret, F. Transformers are rnns: fast autoregressive transformers with linear attention. In *Proceedings of the 37th International Conference on Machine Learning*, ICML’20. JMLR.org, 2020.

Kottapalli, S. R. K., Hubli, K., Chandrashekara, S., Jain, G., Hubli, S., Botla, G., and Doddaiyah, R. Foundation models for time series: A survey. *arXiv preprint arXiv:2504.04011*, 2025.

Li, C., Li, M., and Diao, R. TVNet: A novel time series analysis method based on dynamic convolution and 3d-variation. In *The Thirteenth International Conference on Learning Representations*, 2025. URL <https://openreview.net/forum?id=MZDdTzN6Cy>.

Liang, Y., Wen, H., Nie, Y., Jiang, Y., Jin, M., Song, D., Pan, S., and Wen, Q. Foundation models for time series analysis: A tutorial and survey. In *Proceedings of the 30th ACM SIGKDD conference on knowledge discovery and data mining*, pp. 6555–6565, 2024.

Lieber, O., Lenz, B., Bata, H., Cohen, G., Osin, J., Dalmedigos, I., Safahi, E., Meirom, S., Belinkov, Y., Shalev-Shwartz, S., et al. Jamba: A hybrid transformer-mamba language model. *arXiv preprint arXiv:2403.19887*, 2024.

Liu, C., Aksu, T., Liu, J., Liu, X., Yan, H., Pham, Q., Savarese, S., Sahoo, D., Xiong, C., and Li, J. Moirai 2.0: When less is more for time series forecasting, 2025a. URL <https://arxiv.org/abs/2511.11698>.

Liu, M., Zeng, A., Chen, M., Xu, Z., LAI, Q., Ma, L., and Xu, Q. SCINet: Time series modeling and forecasting with sample convolution and interaction. In Oh, A. H., Agarwal, A., Belgrave, D., and Cho, K. (eds.), *Advances in Neural Information Processing Systems*, 2022a. URL <https://openreview.net/forum?id=AyaJSjTAzmg>.

Liu, S., Yu, H., Liao, C., Li, J., Lin, W., Liu, A. X., and Dustdar, S. Pyraformer: Low-complexity pyramidal attention for long-range time series modeling and forecasting. In *International Conference on Learning Representations*, 2022b. URL <https://openreview.net/forum?id=0EXmFzUn5I>.

Liu, Y., Ott, M., Goyal, N., Du, J., Joshi, M., Chen, D., Levy, O., Lewis, M., Zettlemoyer, L., and Stoyanov, V. Roberta: A robustly optimized bert pretraining approach. *arXiv preprint arXiv:1907.11692*, 2019.

Liu, Y., Zhang, H., Li, C., Huang, X., Wang, J., and Long, M. Timer: Generative pre-trained transformers are large time series models. In *Forty-first International Conference on Machine Learning*, 2024. URL <https://openreview.net/forum?id=bYRYb7DMNo>.

Liu, Y., Qin, G., Huang, X., Wang, J., and Long, M. Timer-XL: Long-context transformers for unified time series forecasting. In *The Thirteenth International Conference on Learning Representations*, 2025b. URL <https://openreview.net/forum?id=KMCJXj1DDr>.

Liu, Y., Qin, G., Shi, Z., Chen, Z., Yang, C., Huang, X., Wang, J., and Long, M. Sundial: A family of highly capable time series foundation models. In *Forty-second*

International Conference on Machine Learning, 2025c. URL <https://openreview.net/forum?id=LO7ciRpjI5>.

Loshchilov, I. and Hutter, F. Decoupled weight decay regularization. In *International Conference on Learning Representations*, 2019. URL <https://openreview.net/forum?id=Bkg6RiCqY7>.

Luo, D. and Wang, X. ModernTCN: A modern pure convolution structure for general time series analysis. In *The Twelfth International Conference on Learning Representations*, 2024. URL <https://openreview.net/forum?id=vpJMJerXHU>.

Ma, H., Chen, Y., Zhao, W., Yang, J., Ji, Y., Xu, X., Liu, X., Jing, H., Liu, S., and Yang, G. A mamba foundation model for time series forecasting. *arXiv preprint arXiv:2411.02941*, 2024.

Massaroli, S., Poli, M., Fu, D. Y., Kumbong, H., Parnichkun, R. N., Romero, D. W., Timalsina, A., McIntyre, Q., Chen, B., Rudra, A., Zhang, C., Re, C., Ermon, S., and Bengio, Y. Laughing hyena distillery: Extracting compact recurrences from convolutions. In *Thirty-seventh Conference on Neural Information Processing Systems*, 2023. URL <https://openreview.net/forum?id=OWELckerm6>.

Moroshan, V., Siems, J., Zela, A., Carstensen, T., and Hutter, F. Tempopfn: Synthetic pre-training of linear rnns for zero-shot time series forecasting, 2025. URL <https://arxiv.org/abs/2510.25502>.

Nie, Y., Nguyen, N. H., Sinthong, P., and Kalagnanam, J. A time series is worth 64 words: Long-term forecasting with transformers. In *The Eleventh International Conference on Learning Representations*, 2023. URL <https://openreview.net/forum?id=Jbdc0vT0col>.

Nochumsohn, L., Marshanski, R., Zisling, H., and Azencot, O. Super-linear: A lightweight pretrained mixture of linear experts for time series forecasting, 2025. URL <https://arxiv.org/abs/2509.15105>.

Quab, M., Darzet, T., Moutakanni, T., Vo, H., Szafraniec, M., Khalidov, V., Fernandez, P., Haziza, D., Massa, F., El-Nouby, A., et al. Dinov2: Learning robust visual features without supervision. *arXiv preprint arXiv:2304.07193*, 2023.

Peng, H., Pappas, N., Yogatama, D., Schwartz, R., Smith, N. A., and Kong, L. Random feature attention. In *Proceedings of ICLR*, 2021.

Petneházi, G. Recurrent neural networks for time series forecasting. *arXiv preprint arXiv:1901.00069*, 2019.

Poli, M., Massaroli, S., Nguyen, E., Fu, D. Y., Dao, T., Baccus, S., Bengio, Y., Ermon, S., and Ré, C. Hyena hierarchy: Towards larger convolutional language models. *arXiv preprint arXiv:2302.10866*, 2023.

Qin, Y., Song, D., Chen, H., Cheng, W., Jiang, G., and Cottrell, G. A dual-stage attention-based recurrent neural network for time series prediction. *arXiv preprint arXiv:1704.02971*, 2017.

Rasul, K., Ashok, A., Williams, A. R., Khorasani, A., Adamopoulos, G., Bhagwatkar, R., Biloš, M., Ghonia, H., Hassen, N., Schneider, A., et al. Lag-llama: Towards foundation models for time series forecasting. In *RoFoMo: Robustness of Few-shot and Zero-shot Learning in Large Foundation Models*, 2023.

Schlag, I., Irie, K., and Schmidhuber, J. Linear transformers are secretly fast weight programmers. In *International conference on machine learning*, pp. 9355–9366. PMLR, 2021.

Shazeer, N. Glu variants improve transformer. *arXiv preprint arXiv:2002.05202*, 2020.

Siems, J., Carstensen, T., Zela, A., Hutter, F., Pontil, M., and Grazzi, R. Deltaproduct: Improving state-tracking in linear RNNs via householder products. In *The Thirty-ninth Annual Conference on Neural Information Processing Systems*, 2025. URL <https://openreview.net/forum?id=SoRiaijTGr>.

Smith, J. T., Warrington, A., and Linderman, S. Simplified state space layers for sequence modeling. In *The Eleventh International Conference on Learning Representations*, 2023. URL <https://openreview.net/forum?id=Ai8Hw3AXqks>.

Stankeviciute, K., M. Alaa, A., and van der Schaar, M. Conformal time-series forecasting. In Ranzato, M., Beygelzimer, A., Dauphin, Y., Liang, P., and Vaughan, J. W. (eds.), *Advances in Neural Information Processing Systems*, volume 34, pp. 6216–6228. Curran Associates, Inc., 2021. URL https://proceedings.neurips.cc/paper_files/paper/2021/file/312f1ba2a72318edaaa995a67835fad5-Paper.pdf.

Sun, S. and Yu, R. Conformal prediction for time-series forecasting with change points, 2025. URL <https://arxiv.org/abs/2509.02844>.

Sun, Y., Fang, Y., Zhu, Z., Li, J., Liu, Y., Deng, Q., Zhou, J., Yu, H., Lu, X., and Ma, L. Xihe: Scalable zero-shot time series learner via hierarchical interleaved block attention, 2025. URL <https://arxiv.org/abs/2510.21795>.

Tan, M., Merrill, M., Gupta, V., Althoff, T., and Hartvigsen, T. Are language models actually useful for time series forecasting? *Advances in Neural Information Processing Systems*, 37:60162–60191, 2024.

Vaswani, A., Shazeer, N., Parmar, N., Uszkoreit, J., Jones, L., Gomez, A. N., Kaiser, Ł., and Polosukhin, I. Attention is all you need. In *Advances in Neural Information Processing Systems 30*, pp. 5998–6008. Curran Associates, Inc., 2017. URL <https://proceedings.neurips.cc/paper/2017/file/3f5ee243547dee91fbd053c1c4a845aa-Paper.pdf>.

Waleffe, R., Byeon, W., Riach, D., Norick, B., Korthikanti, V., Dao, T., Gu, A., Hatamizadeh, A., Singh, S., Narayanan, D., et al. An empirical study of mamba-based language models. *arXiv preprint arXiv:2406.07887*, 2024.

Wang, S., Wu, H., Shi, X., Hu, T., Luo, H., Ma, L., Zhang, J. Y., and Zhou, J. Timemixer: Decomposable multi-scale mixing for time series forecasting. *arXiv preprint arXiv:2405.14616*, 2024.

Wang, X., Zhou, T., Gao, J., Ding, B., and Zhou, J. Output scaling: Yinglong-delayed chain of thought in a large pretrained time series forecasting model, 2025. URL <https://arxiv.org/abs/2506.11029>.

Wen, K., Li, Z., Wang, J. S., Hall, D. L. W., Liang, P., and Ma, T. Understanding warmup-stable-decay learning rates: A river valley loss landscape view. In *The Thirteenth International Conference on Learning Representations*, 2025. URL <https://openreview.net/forum?id=m51BgoqvBP>.

Wen, Y., Gifford, W. M., Reddy, C., Nguyen, L. M., Kalagnanam, J., and Julius, A. A. Revisiting the generic transformer: Deconstructing a strong baseline for time series foundation models, 2026. URL <https://arxiv.org/abs/2602.06909>.

Woo, G., Liu, C., Kumar, A., Xiong, C., Savarese, S., and Sahoo, D. Unified training of universal time series forecasting transformers, 2024. URL <https://arxiv.org/abs/2402.02592>.

Wu, H., Xu, J., Wang, J., and Long, M. Autoformer: Decomposition transformers with auto-correlation for long-term series forecasting. In Beygelzimer, A., Dauphin, Y., Liang, P., and Vaughan, J. W. (eds.), *Advances in Neural Information Processing Systems*, 2021. URL <https://openreview.net/forum?id=I55UqU-M11y>.

Yang, S., Wang, B., Shen, Y., Panda, R., and Kim, Y. Gated linear attention transformers with hardware-efficient training. In *Forty-first International Conference on Machine Learning*, 2024a. URL <https://openreview.net/forum?id=ia5XvxFUJT>.

Yang, S., Wang, B., Zhang, Y., Shen, Y., and Kim, Y. Parallelizing linear transformers with the delta rule over sequence length. In *Proceedings of NeurIPS*, 2024b.

Yang, S., Kautz, J., and Hatamizadeh, A. Gated delta networks: Improving mamba2 with delta rule. In *The Thirteenth International Conference on Learning Representations*, 2025. URL <https://openreview.net/forum?id=r8H7xhYPwz>.

Zeng, A., Chen, M., Zhang, L., and Xu, Q. Are transformers effective for time series forecasting? In *Proceedings of the AAAI Conference on Artificial Intelligence*, 2023.

Zhou, H., Zhang, S., Peng, J., Zhang, S., Li, J., Xiong, H., and Zhang, W. Informer: Beyond efficient transformer for long sequence time-series forecasting, 2021. URL <https://arxiv.org/abs/2012.07436>.

Zhou, T., Ma, Z., Wen, Q., Wang, X., Sun, L., and Jin, R. Fedformer: Frequency enhanced decomposed transformer for long-term series forecasting, 2022. URL <https://arxiv.org/abs/2201.12740>.

Zhou, T., Niu, P., Sun, L., Jin, R., et al. One fits all: Power general time series analysis by pretrained lm. *Advances in neural information processing systems*, 36:43322–43355, 2023.

A. Data generation and augmentation details

A.1. Synthetic data composition

Algorithm 1 KernelSynth Data Generation

Require: Length L , Kernel bank \mathcal{K} (e.g., RBF, Periodic, Linear, Rational Quadratic), Max kernels $J_{max} = 5$.

```

1: Compose Kernel  $\tilde{\kappa}$ :
2: Sample number of kernels  $N \sim \text{Uniform}\{1, J_{max}\}$ 
3: Sample base kernel  $\tilde{\kappa} \sim \mathcal{K}$ 
4: for  $i = 2$  to  $N$  do
5:   Sample next kernel  $k' \sim \mathcal{K}$ 
6:   Sample operation  $\oplus \sim \{\text{Add, Multiply}\}$ 
7:    $\tilde{\kappa} \leftarrow \tilde{\kappa} \oplus k'$ 
8: end for
9: Define Mean Function  $\mu(t)$ :
10: if  $u \sim U(0, 1) < 0.5$  then
11:   Linear trend: Sample  $m \sim U[-0.01, 0.01]$ ,  $c \sim U[-0.1, 0.1]$ 
12:    $\mu(t) = m \cdot t + c$ 
13: else
14:   Constant:  $\mu(t) = 0$  (or sample constant  $c$ )
15: end if
16: Sample Time Series from Gaussian Process:
17: Compute covariance matrix  $\Sigma \in \mathbb{R}^{L \times L}$  where  $\Sigma_{uv} = \tilde{\kappa}(u, v)$ 
18: Compute mean vector  $\mathbf{m} \in \mathbb{R}^L$  where  $\mathbf{m}_t = \mu(t)$ 
19: Sample  $t_{syn} \sim \mathcal{N}(\mathbf{m}, \Sigma)$  {Multivariate Gaussian}
20: return  $t_{syn}$ 
```

We make use of standard synthetic data generation practices that has been developed in the community.

KernelSynth([Ansari et al., 2024](#)) introduced the use of Gaussian Process(GP) for synthetic data generation. In particular, we define a kernel bank \mathcal{K} , and sample $j \sim U\{1, 5\}$ kernels from \mathcal{K} and compose them using random binary additive or multiplicative operations. This forms a composite kernel $\tilde{\kappa}$. We also sample μ which follows a linear trend with slope $m \sim U[-0.01, 0.01]$ and intercept $c \sim U[-0.1, 0.1]$ with probability 1/2 and constant otherwise. We then use $\tilde{\kappa}$ and μ in a Gaussian process to sample the synthetic time series t_{syn} according to

$$t_{syn} \sim \text{GaussianProcess}(\mu, \tilde{\kappa}(i_1, i_2)).$$

We use the following sets of kernels in our kernel bank \mathcal{K} as shown in Table 8, applied to points L_{syn} evenly spaced points $x, x' \in [0, 1]$. To enable efficient sampling, we use batched Cholesky decomposition. The constant, linear, RBF and Rational Quadratic kernels were introduced in KernelSynth ([Ansari et al., 2024](#)). The Matern kernel was used in TempoPFN([Moroshan et al., 2025](#)) as a more robust and accurate representation of how GPs can model real world data. We use the following set of periods $\mathcal{P} = \{24, 48, 96, 168, 336, 672, 7, 14, 30, 60, 365, 730, 4, 26, 52, 6, 12, 40, 10\}$ (normalized by time series length L_{syn}) to capture patterns of various timescales.

Beyond GP data, we also include spike processes ([Auer et al., 2025](#); [Moroshan et al., 2025](#); [Feng et al., 2025](#)) and TSI ([Bahrpeyma et al., 2021](#)) as used in Chronos-2 to help in learning simple trends and periodic patterns.

A.2. Data augmentation specifics

Here we present the various data augmentation strategies that we found to have been helpful in improving the data diversity during training. We demonstrate this in a full pipeline detailed in Algorithm 4. Our pipeline applies transformations at both the instance level (sequentially) and the batch level (Mixup).

1. **Downsampling:** To allow the model to learn features across varying temporal resolutions, we downsample the raw time series t by a factor k . This effectively compresses long-term dependencies into the context window L .

Table 8. Kernel Bank \mathcal{K} used for Synthetic Data Generation

Kernel	Formula $\kappa(x, x')$	Hyperparameters
Constant	C	$C = 1$
Linear	$\sigma^2 + x \cdot x'$	$\sigma \in \{0, 1, 10\}$
RBF	$\exp\left(-\frac{\ x-x'\ ^2}{2l^2}\right)$	$l \in \{0.1, 1, 10\}$
Rational Quadratic	$\left(1 + \frac{\ x-x'\ ^2}{2\alpha}\right)^{-\alpha}$	$\alpha \in \{0.1, 1, 10\}$
Matérn	$\frac{2^{1-\nu}}{\Gamma(\nu)} \left(\sqrt{2\nu} \frac{\ x-x'\ }{l}\right)^\nu K_\nu\left(\sqrt{2\nu} \frac{\ x-x'\ }{l}\right)$	$\nu \in \{0.5, 1.5, 2.5\}, l \in \{0.1, 1, 10\}$
Periodic	$\exp(-2 \sin^2(\pi \ x - x'\ /p))$	$p \in \mathcal{P}$

Algorithm 2 Spike Process Generation, adapted from Kairos (Feng et al., 2025)

Require: Length L , Pattern types $\mathcal{T} = \{\text{"inverted_u"}, \text{"spikes"}\}$, Ranges for baseline $[b_{min}, b_{max}]$, period $[p_{min}, p_{max}]$, amplitude $[a_{min}, a_{max}]$, width $[w_{min}, w_{max}]$, and noise $[\sigma_{min}, \sigma_{max}]$.

- 1: **Sample parameters:**
- 2: $type \sim \text{Uniform}(\mathcal{T})$, $b \sim \text{Uniform}(b_{min}, b_{max})$, $p \sim \text{Uniform}\{p_{min}, p_{max}\}$
- 3: $a \sim \text{Uniform}(a_{min}, a_{max})$, $w \sim \text{Uniform}\{w_{min}, w_{max}\}$, $\sigma_\epsilon \sim \text{Uniform}(\sigma_{min}, \sigma_{max})$
- 4: **Construct trapezoid shape e of length w :**
- 5: Define $u = \lfloor w/4 \rfloor$, $f = \lfloor w/2 \rfloor$, $d = w - u - f$
- 6: $e_{up} = \text{linspace}(0, a, u)$, $e_{flat} = \text{constant}(a, f)$, $e_{down} = \text{linspace}(a, 0, d)$
- 7: $e = [e_{up}; e_{flat}; e_{down}]$
- 8: **Initialize series:** $x_t = b$ for $t = 1, \dots, L$
- 9: $s = -1$ if $type = \text{"inverted_u"}$ else 1
- 10: **Add periodic patterns:**
- 11: **for** $i = 0, p, 2p, \dots < L$ **do**
- 12: $len = \min(w, L - i)$
- 13: $x_{i:i+len} \leftarrow x_{i:i+len} + s \cdot e_{1:len}$
- 14: **end for**
- 15: **Add white noise:** $x \leftarrow x + \epsilon$, where $\epsilon \sim \mathcal{N}(0, \sigma_\epsilon^2)$
- 16: **return** x

2. **Amplitude Modulation:** We multiply t by a piecewise linear function. We follow the implementation from TiReX but sample just a single intermediate changepoint.
3. **Flips:** We apply random sign flips (inverting the y-axis) and temporal reversals (flipping the x-axis). This follows the implementation of TempoPFN (Moroshan et al., 2025).
4. **Censoring:** The series is clipped from both the top and the bottom. This effectively applies a per-sample thresholding which reduces the effect of anomalies on training.
5. **Batch Mixup:** We apply Mixup (Ansari et al., 2024) at the batch level, creating a convex interpolation between samples.

The formal procedure for generating a single training batch is detailed in Algorithm 4.

Algorithm 3 TSI (Trend, Seasonality, Irregularity) Generation, following Chronos-2([Ansari et al., 2025](#))

Require: Length L , Component probabilities $P_{trend}, P_{seas}, P_{noise}, P_{out}, P_{shift}$, Trend types \mathcal{T} , Seasonality periods \mathcal{P} , Wave shapes \mathcal{W} , Noise distributions \mathcal{D} .

- 1: **Initialize:** $x_t \leftarrow 0$ for $t = 1, \dots, L$
- 2: **Add Trend:**
- 3: **if** $u \sim U(0, 1) < P_{trend}$ **then**
- 4: Sample trend type $\tau \in \mathcal{T}$ (e.g., linear, exp, poly, piecewise)
- 5: Sample parameters θ_τ (slope, intercept, degree, etc.)
- 6: $x \leftarrow x + f_\tau(t; \theta_\tau)$
- 7: **end if**
- 8: **Add Seasonality:**
- 9: **if** $u \sim U(0, 1) < P_{seas}$ **then**
- 10: Sample number of components $K \sim U\{1, 3\}$
- 11: Sample distinct periods $\{p_1, \dots, p_K\} \subset \mathcal{P}$
- 12: **for** $k = 1$ to K **do**
- 13: Sample wave form $w \in \mathcal{W}$ (e.g., sine, sawtooth, square)
- 14: Sample amplitude A and phase ϕ
- 15: $x_t \leftarrow x_t + A \cdot w\left(\frac{2\pi}{p_k}t + \phi\right)$
- 16: **end for**
- 17: **end if**
- 18: **Add Irregularity (Noise):**
- 19: **if** $u \sim U(0, 1) < P_{noise}$ **then**
- 20: Sample distribution $\mathcal{N} \in \mathcal{D}$ and scale σ
- 21: $x \leftarrow x + \epsilon$, where $\epsilon \sim \mathcal{N}(0, \sigma)$
- 22: **end if**
- 23: **Add Anomalies:**
- 24: **if** $u \sim U(0, 1) < P_{out}$ **then**
- 25: Add random sparse outliers to x
- 26: **end if**
- 27: **if** $u \sim U(0, 1) < P_{shift}$ **then**
- 28: Add random level shifts (step functions) to x
- 29: **end if**
- 30: **return** x

Algorithm 4 Pretraining Data Augmentation Pipeline

Input: Dataset \mathcal{D} , Batch size B , Context length L
Hyperparameters:

$p(\text{downsample})$, $[k_{min}, k_{max}]$ (Downsample probability, range of downsample ratios)
 $p(\text{modulate})$, $p(\text{flip-x})$, $p(\text{flip-y})$ (Amp. Mod., Flip- x , Flip- y probabilities)
 $p(\text{censor})$ (Censor prob), α (Mixup beta param)

 Initialize batch $\mathcal{B} \leftarrow \emptyset$
while $|\mathcal{B}| < B$ **do**

 Sample raw time series X from \mathcal{D}

{1. Multi-scale Downsampling}

if sample $u \sim U(0, 1) < p_d$ **then**

 Sample stride $k \sim U_{\text{int}}(k_{min}, k_{max})$
 $X \leftarrow \text{Downsample}(X, k)$
end if

{2. Amplitude Modulation}

if sample $u \sim U(0, 1) < p(\text{modulate})$ **then**

 Sample changepoint $x_2 \subset \{1, \dots, \text{len}(X) - 2\}$. Set $x_1 = 0, x_3 = \text{len}(X) - 1$

 Sample scalar $\{y_1, y_2, x_3\} \sim \mathcal{N}(1, 0.5)$

 Piecewise linear $f(x)$ connecting $(x_1, y_1), (x_2, y_2), (x_3, y_3)$
 $X \leftarrow X \cdot f(x)$
end if

{3. Slicing to context length}

 $T_{len} \leftarrow \text{len}(X)$
if $T_{len} > L$ **then**

 Sample $t_{start} \sim U_{\text{int}}(0, T_{len} - L)$
 $x_{seq} \leftarrow X[t_{start} : t_{start} + L]$ (on the next iteration we start at $t_{start} + L$).

else
 $x_{seq} \leftarrow \text{Pad}(X, L)$
end if

{4. Flip Augmentations}

if sample $u \sim U(0, 1) < p(\text{flip-y})$ **then**
 $x_{seq} \leftarrow -x_{seq}$ {Sign Inversion}

end if
if sample $u \sim U(0, 1) < p(\text{flip-x})$ **then**
 $x_{seq}[i] \leftarrow x_{seq}[L - i - 1]$ {Temporal Reversal}

end if

{5. Censor Augmentation}

if sample $u \sim U(0, 1) < p(\text{censor})$ **then**

 Sample $q \sim U(0, 1)$

 Compute threshold $c \leftarrow \text{Quantile}(x_{seq}, q)$

 direction $\sim \{\text{top}, \text{bottom}, \text{none}\}$
if direction = top **then**
 $x_{seq} \leftarrow \min(x_{seq}, c)$
else if direction = bottom **then**
 $x_{seq} \leftarrow \max(x_{seq}, c)$
end if
end if

 Add x_{seq} to \mathcal{B}
end while

{6. Mixup}

 Construct permutation π of $\{0, \dots, L - 1\}$, $\tilde{\mathcal{B}} = \mathcal{B}[\pi]$

 Sample $\lambda \sim \text{Beta}(\alpha, \alpha)$
for $i = 1$ **to** B **do**

 Sample $\lambda \sim \text{Beta}(\alpha, \alpha)$
 $\mathcal{B}[i] \leftarrow \lambda \mathcal{B}[i] + (1 - \lambda) \tilde{\mathcal{B}}[i]$
end for
return \mathcal{B}

B. Extended results on Gift-Eval

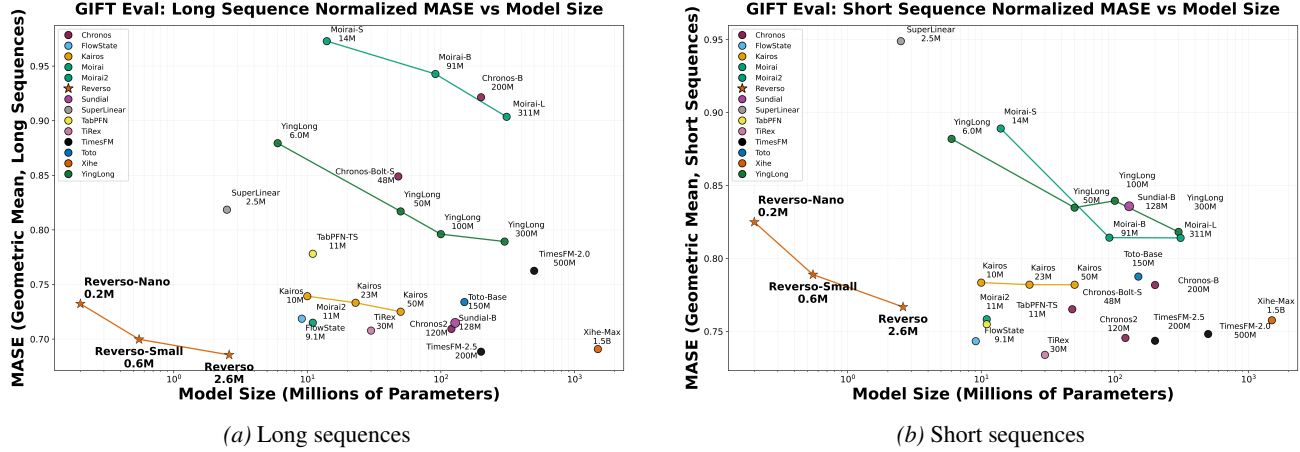


Figure 5. Zero-shot performance on the Gift-Eval benchmark for (a) long sequences (average length at least 2048) and (b) short sequences.

Table 9. Full results on Gift-Eval achieved by Reverso, with an overall MASE of 0.711.

Dataset	Domain	Var	MASE	Dataset	Domain	Var	MASE
loop_seattle/5T/short	Transport	1	0.5531	ett1/H/short	Energy	7	0.8112
loop_seattle/5T/medium	Transport	1	0.8008	ett1/H/medium	Energy	7	1.2476
loop_seattle/5T/long	Transport	1	0.8880	ett1/H/long	Energy	7	1.3336
loop_seattle/D/short	Transport	1	0.8818	ett1/W/short	Energy	7	1.4936
loop_seattle/H/short	Transport	1	0.8113	ett2/15T/short	Energy	7	0.7479
loop_seattle/H/medium	Transport	1	0.9009	ett2/15T/medium	Energy	7	0.8903
loop_seattle/H/long	Transport	1	0.8668	ett2/15T/long	Energy	7	0.9261
m_dense/D/short	Transport	1	0.7038	ett2/D/short	Energy	7	1.3449
m_dense/H/short	Transport	1	0.8146	ett2/H/short	Energy	7	0.7140
m_dense/H/medium	Transport	1	0.6703	ett2/H/medium	Energy	7	0.9900
m_dense/H/long	Transport	1	0.6777	ett2/H/long	Energy	7	0.9873
sz_taxi/15T/short	Transport	1	0.5441	ett2/W/short	Energy	7	0.7538
sz_taxi/15T/medium	Transport	1	0.5420	hierarchical_sales/D/short	Sales	1	0.7456
sz_taxi/15T/long	Transport	1	0.5148	hierarchical_sales/W/short	Sales	1	0.7469
sz_taxi/H/short	Transport	1	0.5698	hospital/M/short	Healthcare	1	0.7863
bitbrains_fast_storage/5T/short	Web/CloudOps	2	0.6703	jena_weather/10T/short	Nature	21	0.2907
bitbrains_fast_storage/5T/medium	Web/CloudOps	2	0.9883	jena_weather/10T/medium	Nature	21	0.6179
bitbrains_fast_storage/5T/long	Web/CloudOps	2	0.8828	jena_weather/10T/long	Nature	21	0.6427
bitbrains_fast_storage/H/short	Web/CloudOps	2	1.0029	jena_weather/D/short	Nature	21	1.3003
bitbrains_rnd/5T/short	Web/CloudOps	2	1.6286	jena_weather/H/short	Nature	21	0.5126
bitbrains_rnd/5T/medium	Web/CloudOps	2	4.3766	jena_weather/H/medium	Nature	21	0.7812
bitbrains_rnd/5T/long	Web/CloudOps	2	3.3422	jena_weather/H/long	Nature	21	1.0075
bitbrains_rnd/H/short	Web/CloudOps	2	5.8132	kdd_cup_2018/D/short	Nature	1	1.2126
bizitobs_application/10S/short	Web/CloudOps	2	1.0614	kdd_cup_2018/H/short	Nature	1	0.9513
bizitobs_application/10S/medium	Web/CloudOps	2	1.5193	kdd_cup_2018/H/medium	Nature	1	1.0454
bizitobs_application/10S/long	Web/CloudOps	2	3.2373	kdd_cup_2018/H/long	Nature	1	1.0415
bizitobs_l2c/5T/short	Web/CloudOps	7	0.2825	m4_daily/D/short	Econ/Fin	1	3.3280
bizitobs_l2c/5T/medium	Web/CloudOps	7	0.4683	m4_hourly/H/short	Econ/Fin	1	0.7820
bizitobs_l2c/5T/long	Web/CloudOps	7	0.4891	m4_monthly/M/short	Econ/Fin	1	0.9472
bizitobs_l2c/H/short	Web/CloudOps	7	0.4383	m4_quarterly/Q/short	Econ/Fin	1	1.2159
bizitobs_l2c/H/medium	Web/CloudOps	7	0.4881	m4_weekly/W/short	Econ/Fin	1	2.0522
bizitobs_l2c/H/long	Web/CloudOps	7	0.5473	m4_yearly/A/short	Econ/Fin	1	3.4251
bizitobs_service/10S/short	Web/CloudOps	2	0.7725	restaurant/D/short	Sales	1	0.6936
bizitobs_service/10S/medium	Web/CloudOps	2	0.9605	saugeen/D/short	Nature	1	2.8601
bizitobs_service/10S/long	Web/CloudOps	2	1.3776	saugeen/M/short	Nature	1	0.7681
car_parts/M/short	Sales	1	0.8652	saugeen/W/short	Nature	1	1.2569
covid_deaths/D/short	Healthcare	1	34.3613	solar/10T/short	Energy	1	1.1669
electricity/15T/short	Energy	1	1.0297	solar/10T/medium	Energy	1	0.8224
electricity/15T/medium	Energy	1	0.8463	solar/10T/long	Energy	1	0.8593
electricity/15T/long	Energy	1	0.8917	solar/D/short	Energy	1	1.0168
electricity/D/short	Energy	1	1.4781	solar/H/short	Energy	1	0.8386
electricity/H/short	Energy	1	0.9649	solar/H/medium	Energy	1	0.8806
electricity/H/medium	Energy	1	1.0626	solar/H/long	Energy	1	0.9416
electricity/H/long	Energy	1	1.1940	solar/W/short	Energy	1	1.4687
electricity/W/short	Energy	1	1.6038	temperature_rain/D/short	Nature	1	1.3853
ett1/15T/short	Energy	7	0.6924	us_births/D/short	Healthcare	1	0.3505
ett1/15T/medium	Energy	7	1.0419	us_births/M/short	Healthcare	1	0.7934
ett1/15T/long	Energy	7	1.0498	us_births/W/short	Healthcare	1	1.0961
ett1/D/short	Energy	7	1.6066				

Table 10. MASE scores versus parameter size breakdowns for models compared in Figure 1. Note that the data leaked version of Chronos-2 has been trained on datasets within Gift-Eval and hence is not included within Figure 1 for fair zero-shot comparison, but is still a strong frame of reference for SOTA foundation models.

Family	Model	Params	MASE
TimesFM	TimesFM-2.5	200M	0.705
	TimesFM-2.0	500M	0.758
PatchTST-FM-r1	PatchTST-FM	260M	0.707
Xihe	Xihe-Max	1.5B	0.711
	Xihe-Base	700M	0.718
	Xihe-Flash	300M	0.726
	Xihe-Lite	94M	0.729
	Xihe-Tiny	9.5M	0.766
Reverso	Reverso	2.6M	0.711
	Reverso-Small	0.6M	0.726
	Reverso-Nano	0.2M	0.760
TiRex	TiRex	30M	0.716
Chronos	Chronos2(Data leakage)	120M	0.698
	Chronos2	120M	0.720
	Chronos-Bolt-S	48M	0.822
	Chronos-B	200M	0.876
FlowState	FlowState-9.1M	9.1M	0.726
	FlowState-2.6M	2.6M	0.735
Kairos	Kairos-50M	50M	0.742
	Kairos-23M	23M	0.748
	Kairos-10M	10M	0.753
Toto	Toto-Base	150M	0.750
Sundial	Sundial-B	128M	0.750
TTM	TTM-Finetuned	1.0M	0.756
TabPFN	TabPFN-TS	11M	0.771
YingLong	YingLong-300M	300M	0.798
	YingLong-110M	100M	0.809
	YingLong-50M	50M	0.822
	YingLong-6M	6.0M	0.880
SuperLinear	SuperLinear	2.5M	0.857
Moirai	Moirai-L	311M	0.875
	Moirai-B	91M	0.901
	Moirai-S	14M	0.946
	Moirai2	11M	0.728

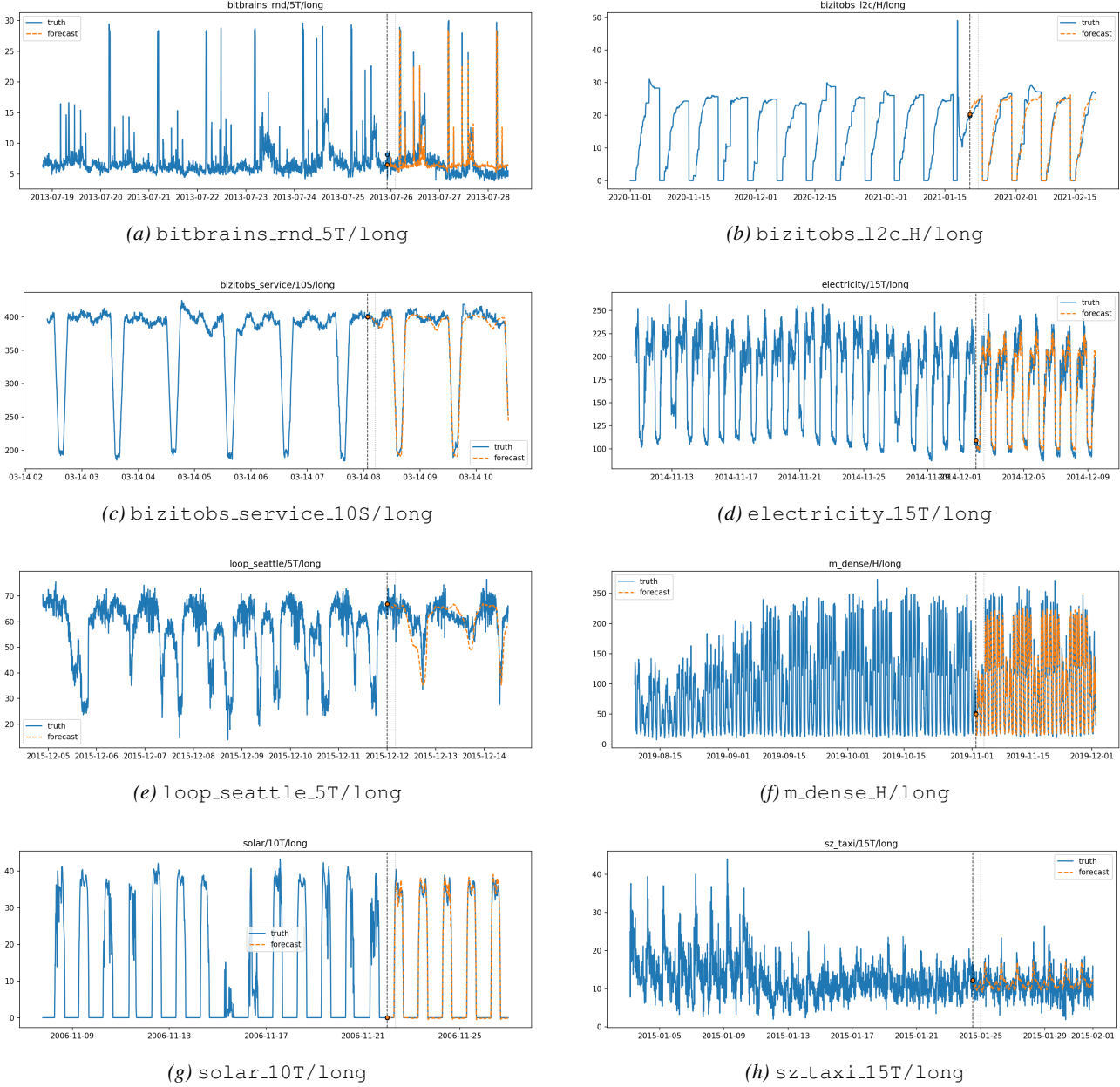


Figure 6. Qualitative results visualizing zero-shot forecasts by Reverso on various tasks within Gift-Eval. Reverso is able to perform long horizon forecasting, accurately capturing patterns at multiple frequency scales. The grey vertical dotted line denotes the length of a single autoregressive prediction.

Table 11. Datasets used for Figure 2, a subset of GiftEval which has all three short/medium/long forecasting horizons.

Dataset	Frequency
bitbrains_fast_storage	5T
bitbrains_rnd	5T
bizitobs_application	10S
bizitobs_l2c	5T
bizitobs_l2c	H
bizitobs_service	10S
electricity	15T
electricity	H
ett1	15T
ett1	H
ett2	15T
ett2	H
jena_weather	10T
jena_weather	H
kdd_cup_2018	H
loop_seattle	5T
loop_seattle	H
m_dense	H
solar	10T
solar	H
sz_taxi	15T

C. Detailed results for LTSF/TSLib

Table 12. Results across each dataset for the models in Figure 4, averaged across the horizons $\{96, 192, 336, 720\}$. Red values represent missing data, imputed using the best available model across each horizon.

Family	Model	Params	ETTh1	ETTh2	ETTm1	ETTm2	Elec.	Weather	Avg
Chronos	Chronos2-120M	120M	0.405	0.367	0.359	0.291	0.237	0.245	0.317
	Chronos-B	200M	0.468	0.410	0.500	0.350	0.279	0.315	0.387
YingLong	YingLong-300M	300M	0.407	0.370	0.358	0.296	0.237	0.245	0.319
	YingLong-110M	110M	0.408	0.366	0.356	0.296	0.237	0.255	0.320
	YingLong-50M	50M	0.408	0.370	0.366	0.298	0.237	0.257	0.323
	YingLong-6M	6.0M	0.412	0.382	0.368	0.302	0.237	0.268	0.328
Reverso	Reverso	2.6M	0.404	0.365	0.367	0.304	0.238	0.253	0.322
	Reverso-Small	0.6M	0.404	0.370	0.376	0.309	0.241	0.252	0.325
	Reverso-Nano	0.3M	0.416	0.384	0.382	0.311	0.249	0.257	0.333
TiRex	TiRex-30M	30M	0.417	0.362	0.365	0.302	0.240	0.247	0.322
PatchTST	PatchTST	5.0M	0.431	0.379	0.381	0.315	0.237	0.264	0.334
VisionTS	VisionTS	112M	0.414	0.375	0.372	0.321	0.237	0.292	0.335
Sundial	Sundial-L	444M	0.419	0.387	0.369	0.315	0.262	0.275	0.338
	Sundial-S	32M	0.418	0.387	0.388	0.324	0.265	0.271	0.342
	Sundial-B	128M	0.434	0.387	0.377	0.320	0.265	0.270	0.342
SuperLinear	Super-Linear	2.5M	0.415	0.386	0.388	0.325	0.267	0.275	0.343
TimesFM	TimesFM	200M	0.444	0.406	0.419	0.347	0.237	0.222	0.346
Moirai	Moirai-B	91M	0.419	0.382	0.385	0.337	0.275	0.282	0.347
Timer	Timer-XL	84M	0.417	0.388	0.392	0.336	0.268	0.294	0.349
Time-MoE	Time-MoE-L	453M	0.420	0.415	0.406	0.361	0.237	0.300	0.356
	Time-MoE-B	113M	0.424	0.404	0.415	0.365	0.237	0.297	0.357

D. Downsampling Algorithm

Algorithm 5 Downsampling

Require: Time series x , Context length L .

Require: Hyperparameters: Dominance ratio α , Significance threshold β , Min periods in window M .

- 1: Compute amplitude spectrum $A(f) = |\text{FFT}(x)|$
- 2: Identify peaks: $p_1 \leftarrow \max_{f>0} A(f)$ at frequency f_1 , $p_2 \leftarrow \max_{f>0, f \neq f_1} A(f)$
- 3: Compute stats: $p_{DC} \leftarrow A(0)$, $\mu_A \leftarrow \text{mean}(A)$, $\sigma_A \leftarrow \text{std}(A)$
- 4: **Check Seasonality Significance:**
- 5: **if** $p_1 \geq \alpha \cdot p_2$ **and** $p_1 \geq p_{DC}$ **and** $p_1 \geq \mu_A + \beta \cdot \sigma_A$ **then**
- 6: Calculate primary period $S \leftarrow 1/f_1$
- 7: Compute stride $k \leftarrow \lfloor \frac{M \cdot S}{L} \rfloor$
- 8: **if** $k > 1$ **then**
- 9: **return** Downsampled series $x' = [x_0, x_k, x_{2k}, \dots]$
- 10: **end if**
- 11: **end if**
- 12: **return** Original series x

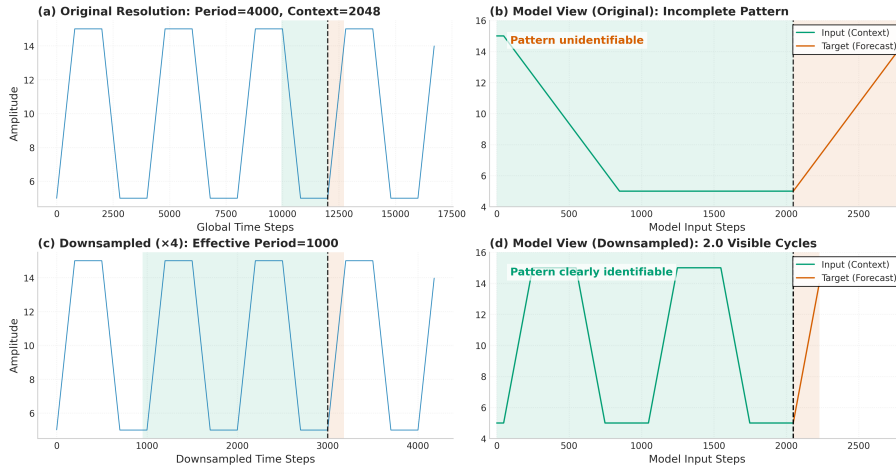


Figure 7. Downsampling Comparison. In this example, consider an input with period 4000 to a model with context length 2048, tasked with forecasting the next 720 points. In (b), the model does not have enough information to forecast the rising part of the trapezoid. However, through downsampling the input, multiple full periods now fit into the context window and the model can forecast more accurately.

Let p_1 be the amplitude of the highest peak at frequency f_1 , and p_2 be the amplitude of the second highest peak. Let p_{DC} denote the DC component (amplitude at $f = 0$), and let μ_A, σ_A be the mean and standard deviation of the spectral amplitudes, respectively. We consider the seasonality at f_1 significant if and only if all the following conditions are met:

$$p_1 \geq \alpha \cdot p_2 \quad (1)$$

$$p_1 \geq p_{DC} \quad (2)$$

$$p_1 \geq \mu_A + \beta \cdot \sigma_A \quad (3)$$

Equation 1 ensures a single dominant frequency exists, mitigating ambiguity from multi-scale seasonality which we leave for future work. Equation 2 ensures the seasonality is stronger than the trend component, and Equation 3 provides statistical confidence that the signal is not merely noise.

If these conditions are satisfied, we calculate the primary period $S = 1/f_1$. To ensure the model captures sufficient temporal

context, we compute a downsampling stride k such that at least M full periods fit within the fixed context window L :

$$k = \left\lfloor \frac{MS}{L} \right\rfloor \quad (4)$$

The input sequence is then downsampled by taking every k -th point, effectively expanding the receptive field of the model to cover $k \cdot L$ time steps while maintaining the fixed input dimension L . If the spectral peaks do not meet the criteria, we do not downsample. We find that typically applying this downsampling algorithm to single time series samples at each time has high variance, resulting in different downsampling ratios for each sequence and in practice we average the downsampling ratios across the same frequency within the same dataset. We use $\alpha = 2, \beta = 4, M = 8$. Downsampling is not applied to short term forecast for which the forecast horizon is significantly shorter than the seasonality since this reduces the resolution of the predictions without capturing further seasonality information.